



Universiteit
Leiden
The Netherlands

Rotational spectroscopy and astronomical search for the 2-hydroxyacetonitrile isotopologues HO¹³CH₂CN, HOCH₂¹³CN, and DOCH₂CN

Margulès, L.; Coutens, A.; Ligterink, N.F.W.; Ahmadi, A.; Motiyenko, R.A.; Alekseev, E.A.; ... ; Guillemin, J.-C.

Citation

Margulès, L., Coutens, A., Ligterink, N. F. W., Ahmadi, A., Motiyenko, R. A., Alekseev, E. A., ... Guillemin, J. -C. (2023). Rotational spectroscopy and astronomical search for the 2-hydroxyacetonitrile isotopologues HO¹³CH₂CN, HOCH₂¹³CN, and DOCH₂CN. *Monthly Notices Of The Royal Astronomical Society*, 524(1), 1211-1218.
doi:10.1093/mnras/stad1834

Version: Publisher's Version

License: [Creative Commons CC BY 4.0 license](https://creativecommons.org/licenses/by/4.0/)

Downloaded from: <https://hdl.handle.net/1887/3717204>

Note: To cite this publication please use the final published version (if applicable).

Rotational spectroscopy and astronomical search for the 2-hydroxyacetonitrile isotopologues $\text{HO}^{13}\text{CH}_2\text{CN}$, $\text{HOCH}_2^{13}\text{CN}$, and DOCH_2CN

L. Margulès,¹★ A. Coutens,^{1,2}★ N. F. W. Ligterink,³ A. Ahmadi,⁴ R. A. Motiyenko,¹ E. A. Alekseev,^{1,5} C. Vastel,² E. Caux² and J.-C. Guillemin⁶★

¹Univ. Lille, PhLAM – Physique des Lasers, Atomes et Molécules, CNRS, UMR 8523, F-59000 Lille, France

²Institut de Recherche en Astrophysique et Planétologie (IRAP), Université de Toulouse, UPS-OMP, CNRS, CNES, 9 av. du Colonel Roche, F-31028 Toulouse Cedex 4, France

³Physics Institute, University of Bern, Sidlerstrasse 5, CH-3012 Bern, Switzerland

⁴Leiden Observatory, Leiden University, PO Box 9513, NL-2300 RA Leiden, the Netherlands

⁵Radioastronomy Department, Institute of Radio Astronomy of NASU, UA-61002 Kharkiv, Ukraine

⁶Univ Rennes, Ecole Nationale Supérieure de Chimie de Rennes, CNRS, ISCR UMR 6226, F-35000 Rennes, France

Accepted 2023 June 8. Received 2023 June 8; in original form 2023 April 6

ABSTRACT

The main isotopologue of 2-hydroxyacetonitrile (glycolonitrile; HOCH_2CN) has recently been detected in the interstellar medium (ISM). To date, no rotational spectroscopy of 2-hydroxyacetonitrile ^{13}C -isotopologues studies has been carried out and only few centimetre-wave measurements of one deuterated isotopologue (DOCH_2CN) exist. The rotational spectrum of the 2-hydroxyacetonitrile ^{13}C -isotopologues and DOCH_2CN was investigated from 150 to 530 GHz. As the parent isotopic species, the other 2-hydroxyacetonitrile isotopologues exhibit large amplitude motion due to the torsion of the hydroxyl group. The analyses of the spectra were carried out using the reduced axis system (RAS) formalism and Watson's S-reduction Hamiltonian implemented in the SPFIT code. More than 3000 lines were fitted for the three studied isotopologues, with quantum number values reaching 60–67 for J and 21–25 for K_a depending on the species. Accurate line lists up to 600 GHz and partition functions are provided. A search for these isotopologues in SMM1-a and IRAS 16293 B surveys resulted in non-detections; upper limits to the column density were determined. The accurate spectroscopic prediction of their spectra provided in this work will allow astronomers to continue the search for 2-hydroxyacetonitrile isotopologues in the ISM.

Key words: astrochemistry – line: identification – molecular data – methods: laboratory: molecular – ISM: molecules – submillimetre: ISM.

1 INTRODUCTION

The astrochemical study of the isotopologues (or isotopomers) of a molecule detected in the interstellar medium (ISM) is an essential tool for improving the understanding of the formation of these compounds by searching for similar isotopic ratios in possible precursors. This approach thus allows to eliminate a number of potential reactants and the reactions associated with them. The remaining precursor(s) allows considering possible chemical reactions which can also lead to other compounds which become target compounds. On Earth, the $^{13}\text{C}/^{12}\text{C}$ ratio is about 1 per cent. This ratio can vary considerably depending on the studied area of the universe. It is of the order of 4–5 per cent in the region of the Galactic Centre, and 1–2 per cent in the Solar neighbourhood (Wilson & Rood 1994; Müller et al. 2008; Halfen, Woolf & Ziurys 2017; Jacob et al. 2020). Similarly, deuterated compounds were observed. Even trideuterated compounds, ND_3 and CD_3OH , were detected, this implies a huge enhancement

factor compared to the deuterium/hydrogen cosmic value (Parise et al. 2004; Roueff et al. 2005). In order to quantify the ratio between isotopologues, laboratory recording of the spectrum of each isotopologue is necessary before detecting them and determining the ratio between each and the main isotopomer if they are sufficiently abundant to perform such studies. We recently reported the millimetre spectrum of 2-hydroxyacetonitrile (HOCH_2CN , glycolonitrile, hereafter hydroxyacetonitrile; Margulès et al. 2017) and this compound was detected a few months later in both the inner hot corino and the outer cold envelope of IRAS 6293 B (Zeng et al. 2019). Later, a second detection of hydroxyacetonitrile was reported towards Serpens SMM1-a (Ligterink et al. 2021). These two detections are thus far the only observations of this molecule. Hydroxyacetonitrile is considered a prebiotic molecule because it is a catalyst for the formation of the nucleobase adenine (Schwartz & Goverde 1982) and is often a by-product in the synthesis by a Strecker reaction of aminoacetonitrile ($\text{NH}_2\text{CH}_2\text{CN}$). It can be formed in the ISM through the reaction of the CN anion or radical with formaldehyde (Danger et al. 2012). Thus, a link can be established between the ratios of the ^{13}C and ^{12}C isotopologues of hydroxyacetonitrile if they

* E-mail: laurent.margules@univ-lille.fr (LM); audrey.coutens@irap.omp.eu (AC); jean-claude.guillemin@ensc-rennes.fr (JCG)

are detected, and those of formaldehyde and hydrogen cyanide in the event that such ratios can be measured for these compounds in the same area. We report here the synthesis, measurements, and analysis of the two ^{13}C isotopomers of ($\text{HO}^{13}\text{CH}_2\text{CN}$ and $\text{HOCH}_2^{13}\text{CN}$) and one deuterated isotopologue (DOCH_2CN) spectra in the range 150–530 GHz.

2 EXPERIMENTAL SECTION

2.1 Synthesis

Paraformaldehyde- ^{13}C and potassium cyanide- ^{13}C were purchased from Eurisotop and used without further purification. Formaldehyde (37 wt per cent in water), potassium cyanide and methanol-*d* (CH_3OD) were purchased from Sigma–Aldrich. 2-hydroxyacetonitrile- $1\text{-}^{13}\text{C}$ and 2-hydroxyacetonitrile- $2\text{-}^{13}\text{C}$ were prepared as previously reported for the main isotopologue (Gaudry 1947, 1955) but using paraformaldehyde- ^{13}C or potassium cyanide- ^{13}C , respectively.

2.1.1 Hydroxyacetonitrile- $2\text{-}^{13}\text{C}$ ($\text{HO}^{13}\text{CCH}_2\text{CN}$)

To obtain 6 g of a 20 wt per cent aqueous solution of ^{13}C -formaldehyde, paraformaldehyde- ^{13}C (1.20 g) was diluted in water (4.8 g) under stirring, heating to 50°C and then cooled at room temperature. In a 50 mL flask cooled to 0°C , potassium cyanide (2.6 g, 40 mmol) was dissolved in water (5 mL) and formaldehyde- ^{13}C (20 per cent in water, 6 g) was added dropwise. After 10 min standing, 4.6 mL of dilute sulfuric acid (1.14 mL, 1.84 g mL^{-1} , in 3.5 mL of water) was added dropwise to the cold solution (0°C). A copious precipitate of potassium sulfate was formed. The pH of the solution was about 1.9. A 10 per cent potassium hydroxide solution was then added, dropwise, and with cooling, until the pH was about 3.0. The flask was then removed from the cooling bath, 10 mL of diethyl ether have been added, and the mixture was well shaken. The salt was removed by filtration, and washed with 5 mL of diethyl ether. 2-Hydroxyacetonitrile- $1\text{-}^{13}\text{C}$ was then extracted ($10 \times 10\text{ mL}$ of diethyl ether), dried, and distilled in vacuo. Yield: 65 per cent. ^1H NMR (CD_3CN , 400 MHz) δ 3.83 (m brd, 1H, OH); 4.29 (dd, 2H, $^2J_{\text{CH}} = ^3J_{\text{HH}} = 6.4\text{ Hz}$, CH_2). ^{13}C NMR (CD_3CN , 100 MHz) δ 48.1 [$^1J_{\text{CH}} = 152.6\text{ Hz}$ (t), CH_2]; 118.7 [d, $^1J_{\text{CC}} = 59.5\text{ Hz}$ (d), CN].

2.1.2 Hydroxyacetonitrile- $1\text{-}^{13}\text{C}$ ($\text{HOCH}_2^{13}\text{CN}$)

The same procedure was used with potassium cyanide- ^{13}C (2.7 g, 40 mmol), water (5 mL), and formaldehyde (3.4 mL, 37 wt per cent in water and 2.6 mL of water). Yield: 65 per cent. ^1H NMR (CD_3CN , 400 MHz) δ 3.83 (m brd, 1H, OH); 4.29 (dd, 2H, $^2J_{\text{CH}} = ^3J_{\text{HH}} = 6.4\text{ Hz}$, CH_2). ^{13}C NMR (CD_3CN , 100 MHz) δ 48.1 [$^1J_{\text{CC}} = 59.5\text{ Hz}$ (d), $^1J_{\text{CH}} = 152.6\text{ Hz}$ (t), CH_2]; 118.7 [$^2J_{\text{CH}} = 6.4\text{ Hz}$ (t), CN].

2.1.3 Deuterioxyacetonitrile (DOCH_2CN)

Methanol-*d* CH_3OD (3.2 g, 0.1 mol) was added to hydroxyacetonitrile (1.14 g, 20 mmol) and the mixture was stirred for 10 min at room temperature. Low boiling compounds were removed in vacuo and the reaction repeated twice.

2.2 Lille: submillimetre wave spectra

The measurements in the frequency range under investigation (150–530 GHz) were performed using the Lille spectrometre (Zakharenko et al. 2015). The absorption cell was a stainless-steel tube (6 cm in diameter, 220 cm in length). The sample pressure and temperature during measurements were about 10 Pa and room temperature, and the linewidth was limited by Doppler broadening. The frequency range 150–530 GHz was covered with various active and passive frequency multipliers from VDI Inc. and an Agilent synthesizer (12.5–18.25 GHz) was used as the source of radiation. Absorption signals were detected by an InSb liquid He-cooled bolometer (QMC Instruments Ltd). Estimated uncertainties for measured line frequencies are 30 and 50 kHz depending on the observed signal-to-noise (S/N) and the frequency range.

3 ANALYSIS OF THE ROTATIONAL SPECTRA

As for the parent isotopic species, we only analysed the spectra of the gauche rotamer, which is the most stable one. The trans rotamer of hydroxyacetonitrile is calculated to be $1.41\text{ kcal mol}^{-1}$ ($493\text{ cm}^{-1}/710\text{ K}$) higher in energy (Dalbouha, Domínguez-Gómez & Senent 2017). The analysis was complicated by a large amplitude motion (LAM) with a symmetric two minima potential due to the two equivalent gauche rotamers. As a result of the tunnelling through the barrier to OH-group torsion, each energy level of 2-hydroxyacetonitrile is split into two substates labelled here as 0 (the lowest energy level) and 1. The corresponding labelling used by Dalbouha et al. (2017) is A1 and A2. The structure of gauche rotamer is very close to a symmetric prolate rotor with an asymmetry parameter $\kappa = -0.968$. Many nitriles are characterized by large dipole moment. It is also the case of 2-hydroxyacetonitrile: $\mu_a = 2.32$, $\mu_b = 1.31$, $\mu_c = 1.23\text{ D}$. These ab initio values are from Dalbouha et al. (2017). It should be noted that the component of the dipole moment along *c*-axis is linked to torsion motion, and allows transitions between the two torsional substates.

For the global fit, a model based on the reduced axis system (RAS) approach proposed by Pickett (1972) was implemented in the widely used SPFIT/SPCAT programmes for fitting and predicting molecular spectra. It has been shown by Christen & Müller (2003) that the RAS formalism is equivalent to the internal axis method (IAM) approaches developed by Hougen and coworkers for molecules with several large amplitude motions (Hougen 1985; Coudert & Hougen 1988). This method is particularly suitable for double minimum LAM cases, we employed it successfully in previous studies (Motiyenko et al. 2010, 2015; Smirnov et al. 2013) and in particular with the hydroxyacetonitrile normal species (Margulès et al. 2017). More details about the model can be found in this paper.

3.1 ^{13}C isotopologues

The analysis of the ^{13}C isotopologues was rather straightforward. Even if no spectroscopic studies existed up to now, we could take benefit of the main isotopologue study. Substituting the ^{12}C with ^{13}C does not affect significantly kinetic and potential energy of LAM as it can be verified in the final parameters set table (Table 1). With this assumption, for both ^{13}C isotopologues, we used as starting parameters the ab initio ground vibrational state rotational constants of Table 2 in Dalbouha et al. (2017) while all the other parameters (centrifugal distortion, tunnelling splitting, and Coriolis coupling constants) were taken from Margulès et al. (2017). The initial predictions obtained using these parameters allowed, for example,

Table 1. Spectroscopic parameters of the ¹³C and deuterated gauche conformer of 2-hydroxyacetonitrile species.

| Parameters in MHz | HOCH ₂ CN ^a | HO ¹³ CH ₂ CN | HOCH ₂ ¹³ CN | DOCH ₂ CN |
|---|-----------------------------------|-------------------------------------|------------------------------------|----------------------|
| Rotational and centrifugal distortion constants | | | | |
| <i>A</i> | 33609.53194(27) ^b | 32787.31228(29) | 33569.30468(40) | 30653.94661(70) |
| <i>B</i> | 4838.014347(41) | 4820.980595(68) | 4810.878790(83) | 4725.725505(99) |
| <i>C</i> | 4377.304462(40) | 4349.083437(65) | 4354.399428(80) | 4262.86028(24) |
| <i>D_J</i> × 10 ³ | 3.093051(44) | 3.008971(76) | 3.049000(80) | 3.280413(94) |
| <i>D_{JK}</i> × 10 ³ | − 63.89803(34) | − 59.85131(51) | − 64.23275(47) | − 54.586(17) |
| <i>D_K</i> × 10 ³ | 969.2208(61) | 917.8160(52) | 982.3170(80) | 753.258(32) |
| <i>d₁</i> × 10 ³ | − 0.695725(10) | − 0.692148(22) | − 0.685525(26) | − 0.788049(46) |
| <i>d₂</i> × 10 ³ | − 0.041757(18) | − 0.043740(23) | − 0.040349(15) | − 0.055228(45) |
| <i>H_J</i> × 10 ⁶ | 0.0107392(81) | 0.010232(23) | 0.010513(28) | 0.011381(31) |
| <i>H_{JK}</i> × 10 ⁶ | − 0.16090(71) | − 0.1265(13) | − 0.17990(54) | 0.2101(91) |
| <i>H_{KJ}</i> × 10 ⁶ | − 3.6005(17) | − 3.4904(44) | − 3.4713(15) | − 5.399(33) |
| <i>H_K</i> × 10 ⁶ | 82.883(56) | 77.670(30) | 83.883(55) | 60.75(11) |
| <i>h₁</i> × 10 ⁶ | 0.0044035(40) | 0.004285(11) | 0.004305(13) | 0.004613(22) |
| <i>h₂</i> × 10 ⁶ | 0.0005288(27) | 0.0005242(20) | 0.0005086(18) | 0.000368(11) |
| <i>h₃</i> × 10 ⁶ | 0.00007335(95) | 0.0000622(12) | 0.00008221(61) | |
| <i>L_K</i> × 10 ⁹ | − 3.14(17) | − 3.14 ^c | − 3.14 ^c | |
| <i>L_{KKJ}</i> × 10 ⁹ | 0.3292(25) | 0.3028(20) | 0.3435(15) | 0.751(18) |
| <i>L_{JK}</i> × 10 ⁹ | − 0.04864(29) | − 0.04450(42) | − 0.04609(63) | 0.000169(33) |
| <i>L_{JJK}</i> × 10 ⁹ | 0.001496(12) | 0.001417(24) | 0.001485(27) | − 0.1871(34) |
| <i>L_J</i> × 10 ⁹ | − 0.00005190(75) | − 0.0000553(28) | − 0.0000624(36) | − 0.0000840(34) |
| <i>l₁</i> × 10 ⁹ | − 0.00002619(46) | − 0.0000298(16) | − 0.0000265(19) | − 0.0000208(26) |
| <i>l₂</i> × 10 ⁹ | − 0.00000544(39) | − 0.00000544 ^c | − 0.00000544 ^c | |
| <i>l₃</i> × 10 ⁹ | − 0.00000236(17) | − 0.00000236 ^c | − 0.00000236 ^c | |
| Tunnelling splitting constants | | | | |
| <i>E</i> | 112672.5526(30) | 112016.5779(41) | 112716.4480(55) | 17567.0493(89) |
| <i>E_J</i> | 1.0954348(39) | 1.0751770(59) | 1.0883325(56) | 0.380161(59) |
| <i>E_K</i> | − 13.606157(53) | − 13.273996(71) | − 13.78242(11) | − 3.71749(19) |
| <i>E_{JJ}</i> × 10 ³ | − 0.00749(11) | − 0.00487(24) | − 0.01055(13) | − 0.007934(35) |
| <i>E_{JK}</i> × 10 ³ | − 0.19132(72) | − 0.2154(14) | − 0.16000(80) | − 0.1601(30) |
| <i>E_{KK}</i> × 10 ³ | 0.44739(78) | 0.4516(14) | 0.3688(14) | 0.1017(35) |
| <i>E₂</i> | 0.331606(22) | 0.329474(47) | 0.329718(27) | 0.119585(35) |
| <i>E_{2J}</i> × 10 ³ | − 0.0073918(30) | − 0.0072687(69) | − 0.0073022(88) | − 0.005092(24) |
| <i>E_{2K}</i> × 10 ³ | 1.339(22) | 1.589(46) | 0.664(26) | 0.3930(43) |
| <i>E_{2JJ}</i> × 10 ⁹ | 0.07826(71) | 0.0935(16) | 0.0928(19) | 0.1222(28) |
| <i>E_{2JK}</i> × 10 ⁹ | − 21.80(20) | − 19.53(34) | − 29.19(32) | − 18.93(28) |
| <i>E₄</i> × 10 ⁶ | − 5.215(60) | − 6.29(12) | − 3.533(63) | − 1.8968(74) |
| <i>E_{4J}</i> × 10 ⁹ | 0.1756(13) | 0.1959(27) | 0.2005(28) | 0.2708(34) |
| Coriolis coupling constants | | | | |
| <i>F_{bc}</i> | − 5.7926(14) | − 5.9589(18) | − 5.77100(11) | − 3.32962(35) |
| <i>F_{bcK}</i> × 10 ³ | 43.41(74) | 56.41(92) | 31.77(59) | − 112.97(28) |
| <i>F_{bcJ}</i> × 10 ³ | − 0.113411(86) | − 0.115675(85) | − 0.11216(10) | − 0.46075(94) |
| <i>F_{bcKK}</i> × 10 ⁶ | − 19.08(43) | − 12.27(24) | − 25.60(32) | 38.69(80) |
| <i>F_{bcJK}</i> × 10 ⁶ | 0.4789(72) | 0.3470(77) | 0.517(11) | |
| <i>F_{bcJJ}</i> × 10 ⁶ | | | | 0.014149(81) |
| <i>F_{2bc}</i> × 10 ⁶ | 86.5(14) | 116.7(19) | 62.3(11) | − 22.135(52) |
| <i>F_{ac}</i> | 75.52596(18) | 73.71299(25) | 75.01253(25) | 136.707(18) |
| <i>F_{acJ}</i> × 10 ³ | − 0.05771(28) | − 0.07313(36) | − 0.05196(44) | |
| <i>F_{acK}</i> × 10 ³ | 9.943(25) | 10.099(30) | 9.835(36) | 19.91(91) |
| <i>F_{acJK}</i> × 10 ⁶ | 0.485(16) | 0.185(16) | 0.193(16) | |
| <i>F_{acKK}</i> × 10 ⁶ | − 9.229(30) | − 8.740(29) | − 8.798(37) | − 34.37(42) |
| Number of distinct lines | 5128 | 3403 | 3235 | 3190 |
| Number of parameters | 47 | 45 | 44 | 44 |
| <i>J</i> _{max} ^{''} , <i>K</i> _{a,max} ^{''} | 75, 25 | 67, 25 | 6326 | 6021 |
| Standard deviation (in kHz) | 29.2 | 26.3 | 28.7 | 26.3 |
| Weighted deviation | 0.931 | 0.855 | 0.916 | 0.875 |

Notes. ^aMargulès et al. (2017). ^bNumber in parentheses is one standard deviation in unit of the last digit. ^cFixed to main isotopologue value.

easy assignment of HO¹³CH₂CN ^a*R*-branch *J* = 17–16 band heads at 156 GHz that were shifted by 260 MHz in the experimental spectrum. The ^a*R* branch transitions are the most intense in the spectra, due to

the large μ_a value. Their assignment and improvement of the set of Hamiltonian parameters permitted the search for *b*-type transitions. Finally, we were also able to assign *c*-type transitions connecting

Table 2. Comparison of experimental and ab initio parameters in MHz.

| Parameters | HO ¹³ CH ₂ CN | | HOCH ₂ ¹³ CN | | DOCH ₂ CN | | Cazzoli et al. ^b |
|------------|-------------------------------------|------------------------|------------------------------------|-----------|----------------------|-----------|-----------------------------|
| | This work | Ab initio ^a | This work | Ab initio | This work | Ab initio | |
| <i>A</i> | 32787.31523(44) ^c | 32800.04 | 33569.30468(40) | 33579.15 | 30653.94661(70) | 30666.47 | 30651.04(22) |
| <i>B</i> | 4820.980561(79) | 4811.81 | 4810.878790(83) | 4801.98 | 4725.725505(99) | 4716.15 | 4726.75(22) |
| <i>C</i> | 4349.083413(75) | 4342.59 | 4354.399428(80) | 4348.01 | 4262.86028(24) | 4255.64 | 4262.36(22) |
| <i>E</i> | 112016.5659(48) | 95334.00 | 112716.4480(55) | 96533.17 | 17567.061(10) | 15.289.42 | 16749.57 |

Notes. ^aDalbouha et al. (2017). ^bCazzoli, Lister & Mirri (1973). ^cNumber in parentheses is one standard deviation in unit of the last digit.

two torsional substates. Going step-by-step with the different ranges (150–220, 225–330, 400–530 GHz) permitted to determine almost all the rotational and tunnelling parameters we could fit in the main isotopologue study (Margulès et al. 2017). The same procedure was used for the second ¹³C isotopologue: HOCH₂¹³CN. Some of the optic distortion constants which could not be determined better than 10 times their standard deviation were kept fixed at the main isotopologue values.

In total, 3403 distinct lines of the HO¹³CH₂CN isotopologue were assigned with maximum values for *J* and *K_a* of 67 and 25, respectively. The standard deviation of the fit is 26.3 kHz and 45 parameters were determined. For HOCH₂¹³CN isotopologue, the data set is composed of 3235 lines with maximum values for *J* and *K_a* of 63 and 26, respectively. The standard deviation of the fit is 28.7 kHz and 44 parameters were determined. The number of parameters needed to reproduce experimental accuracy seems important, but this is generally the case when dealing with large amplitude motion.

The final set of parameters that we obtained are listed in Table 1. The first column of the table shows the parameters of the main isotopologue from Margulès et al. (2017). This permits to check the good agreement of the ¹³C parameters from this new study with the ¹²C ones. From the analysis of Table 1, it can be clearly seen that ¹²C to ¹³C isotopic substitution has a very limited influence on tunnelling Hamiltonian parameters. We also compare in Table 2 the rotational constants *A*, *B*, and *C*, and energy difference between tunnelling sublevels *E* from our study with the ab initio calculations. The difference between theoretical and experimental values for ¹³C isotopologues have the same order of magnitude as for the main isotopologue (see table 2 of Margulès et al. 2017). This confirms the quality of the results obtained in this work.

3.2 Deuterated isotopologue: DOCH₂CN

Despite the existence of centimetre-wave measurements (Cazzoli et al. 1973), the analysis of the DOCH₂CN spectra was more complicated. The deuteration of the hydroxyl group hydrogen implies a significant variation of the mass of the tunnelling atom which has a direct influence on the tunnelling probability and hence on the splitting between 0 and 1 substates, and in general, on the tunnelling dynamics. Therefore, for DOCH₂CN isotopic species, as starting set of tunnelling and Coriolis coupling parameters, we could not use the ones determined for the parent or ¹³C species. The initial assignment and analysis were performed separately for the two tunnelling substates. The initial spectral predictions were calculated with Watson’s Hamiltonian in the *I'* representation, the rotational parameters from Cazzoli et al. (1973), and the ab initio quartic centrifugal distortion constants (Dalbouha et al. 2017). In such manner, we assigned ^a*R*-branch transitions for both substates up to *K_a*'' = 4 in the 150–300 GHz range corresponding to *J*' between 18 and 30. The assignment of higher *K_a* transitions was not possible without taking Coriolis-type interaction between tunnelling substates

into account. However, the least-squares fitting using the global model is not straightforward due to the strong correlation between tunnelling and Coriolis-coupling parameters. In this case, the initial fit strategy is to fix one of the two parameters, the energy difference *E* or the Coriolis coupling parameter *F_{bc}*, to a series of reasonable values, to vary the second one, and to search for a minimum rms deviation solution as a function of fixed parameter Motiyenko et al. (2018). We used *E* as fixed parameter in the range between 15 and 18 GHz that comprises the corresponding values from ab initio calculations, 15.3 GHz, and from an estimation by Cazzoli et al. (1973), 16.7 GHz. Using this strategy, the minimum rms deviation fit was obtained for *E* = 17.5 GHz. New predictions calculated using optimized value of *E* allowed us to locate and assign in the spectra *c*-type transitions that connect two tunnelling substates, and thus, to remove the correlation between tunnelling and Coriolis-coupling parameters. One should note that without accurate estimation of *E*, it is almost impossible to assign correctly *c*-type transitions. For example, the *c*-type transition frequencies calculated using *E* values from Dalbouha et al. (2017) or Cazzoli et al. (1973) are shifted by few GHz compared to experimental positions. Finally, after removing the correlations, we switched to a model that uses a single set of rotational and centrifugal distortion parameters for both substates, as in the case of the parent or ¹³C isotopic species.

A total of 3190 distinct lines of the DOCH₂CN were assigned with maximum values for *J* and *K_a* of 60 and 21, respectively. Among the assigned lines 393 lines are transitions between tunnelling substates. 44 parameters were determined and the standard deviation of the fit is 26.6 kHz. We can observe in the Table 2, a good agreement of the rotational constants and energy difference of the sublevels from our study with the ab initio calculations. As mentioned for ¹³C species, the difference observed have the same order of magnitude as the main isotopologue (Margulès et al. 2017). For example, the energy difference we obtained 17567.061(10) MHz is in good agreement with 15289.4 MHz, regarding the 15 per cent accuracy for the main and ¹³C isotopologues.

Part of the new measurements with the fit residuals for HO¹³CH₂CN, HOCH₂¹³CN, and DOCH₂CN are given in Tables 3, 4, and 5. Owing to their large size, the complete versions of the global fit (Tables S1, S2, and S3) for the three isotopologues are supplied at the CDS.¹ The predicted spectra are available in different formats including STANDARD.CAT format (Pickett 1972) from the new data base of the Lille spectroscopy group called the Lille Spectroscopic Database.² The predictions can be generated using various options (e.g. intensity units, temperature, and frequency range) that provide additional flexibility in the data access.

¹<https://cds.unistra.fr> (description of the VizieR service was published in 2000, A&AS 143, 23).

²<https://lsd.univ-lille.fr> (Lille Spectroscopic Database is created and maintained by Roman Motiyenko and Laurent Margulès).

Table 3. Measured frequencies of the HO¹³CH₂CN isotopologue and residuals from the fit (full fit is available at the CDS: S1).

| J'' | Upper level | | | J' | Lower level | | | Frequency (Unc.) (in MHz) | obs-calc (in MHz) |
|-------|-------------|---------|-----------|------|-------------|--------|---------|------------------------------|----------------------|
| | K''_a | K''_c | $v_t''^a$ | | K'_a | K'_c | v_t^a | | |
| 61 | 1 | 60 | 1 | 60 | 1 | 59 | 1 | 539819.787(0.030) | -0.000 |
| 61 | 2 | 60 | 1 | 60 | 1 | 59 | 1 | 539863.767(0.030) | 0.004 |
| 60 | 3 | 58 | 1 | 59 | 2 | 57 | 1 | 539875.463(0.030) | -0.031 |
| 61 | 1 | 60 | 0 | 60 | 2 | 59 | 0 | 539908.910(0.030) | -0.009 |
| 19 | 7 | 12 | 0 | 18 | 6 | 13 | 0 | 539943.488(0.030) | 0.002 |
| 19 | 7 | 13 | 0 | 18 | 6 | 12 | 0 | 539943.488(0.030) | 0.030 |
| 61 | 2 | 60 | 0 | 60 | 2 | 59 | 0 | 539950.533(0.030) | -0.042 |
| 61 | 1 | 60 | 0 | 60 | 1 | 59 | 0 | 539959.986(0.030) | -0.002 |
| 58 | 4 | 54 | 1 | 57 | 4 | 53 | 1 | 539974.592(0.030) | 0.040 |
| 60 | 3 | 58 | 0 | 59 | 2 | 57 | 0 | 539977.449(0.030) | -0.030 |

Note. ^aFollowing SPFIT format the torsional substates A1 and A2 are labelled 0 and 1, respectively.

Table 4. Measured frequencies of the HOCH₂¹³CN isotopologue and residuals from the fit (full fit is available at the CDS: S2).

| J'' | Upper level | | | J' | Lower level | | | Frequency (Unc.) (in MHz) | o.-c. (in MHz) |
|-------|-------------|---------|-----------|------|-------------|--------|---------|------------------------------|-------------------|
| | K''_a | K''_c | $v_t''^a$ | | K'_a | K'_c | v_t^a | | |
| 45 | 5 | 40 | 0 | 44 | 4 | 40 | 1 | 527413.846(0.03000) | -0.032 |
| 33 | 3 | 30 | 1 | 32 | 2 | 30 | 0 | 527665.846(0.03000) | 0.079 |
| 52 | 4 | 49 | 1 | 51 | 3 | 48 | 1 | 527765.891(0.03000) | 0.036 |
| 58 | 4 | 55 | 1 | 57 | 4 | 54 | 1 | 528239.640(0.03000) | -0.001 |
| 58 | 4 | 55 | 0 | 57 | 4 | 54 | 0 | 528436.677(0.03000) | 0.042 |
| 56 | 8 | 49 | 1 | 56 | 7 | 49 | 0 | 528606.153(0.03000) | -0.063 |
| 17 | 5 | 12 | 1 | 16 | 4 | 12 | 0 | 528611.553(0.03000) | -0.023 |
| 17 | 5 | 13 | 1 | 16 | 4 | 13 | 0 | 528642.147(0.03000) | -0.056 |
| 23 | 6 | 17 | 0 | 22 | 5 | 18 | 0 | 528776.749(0.03000) | 0.047 |
| 23 | 6 | 17 | 1 | 22 | 5 | 18 | 1 | 528984.733(0.03000) | 0.057 |

Note. ^aFollowing SPFIT format the torsional substates A1 and A2 are labelled 0 and 1, respectively.

Table 5. Measured frequencies of the DOCH₂CN isotopologue and residuals from the fit (full fit is available at the CDS: S3).

| J'' | Upper level | | | J' | Lower level | | | Frequency (Unc.) (in MHz) | o.-c. (in MHz) |
|-------|-------------|---------|-----------|------|-------------|--------|---------|------------------------------|-------------------|
| | K''_a | K''_c | $v_t''^a$ | | K'_a | K'_c | v_t^a | | |
| 20 | 7 | 13 | 0 | 19 | 6 | 14 | 0 | 519153.053(0.03000) | -0.021 |
| 20 | 7 | 14 | 0 | 19 | 6 | 13 | 0 | 519153.053(0.03000) | 0.044 |
| 20 | 7 | 13 | 1 | 19 | 6 | 14 | 1 | 519208.530(0.03000) | -0.064 |
| 20 | 7 | 14 | 1 | 19 | 6 | 13 | 1 | 519208.530(0.03000) | 0.000 |
| 30 | 5 | 26 | 1 | 29 | 4 | 26 | 0 | 519570.812(0.03000) | -0.001 |
| 24 | 6 | 18 | 1 | 23 | 5 | 18 | 0 | 519677.999(0.03000) | 0.033 |
| 24 | 6 | 19 | 1 | 23 | 5 | 19 | 0 | 519704.748(0.03000) | 0.066 |
| 57 | 4 | 53 | 1 | 56 | 4 | 52 | 1 | 519765.867(0.03000) | 0.024 |
| 57 | 4 | 53 | 0 | 56 | 4 | 52 | 0 | 519853.924(0.03000) | -0.079 |
| 56 | 4 | 53 | 1 | 55 | 3 | 52 | 1 | 519863.089(0.03000) | 0.012 |
| 59 | 3 | 57 | 0 | 58 | 2 | 56 | 0 | 519888.201(0.03000) | 0.026 |

Note. ^aFollowing SPFIT format the torsional substates A1 and A2 are labelled 0 and 1, respectively.

3.3 Partition function

The tabulated values for the partition function are given in Table 6, with $Q_{\text{tot}}(T) = Q_{\text{vib}}(T) \times Q_{\text{rot}}(T)$. The rotational partition function was obtained directly at various temperatures from SPCAT (Pickett 1991) with J up to 90 and K_a up to 40. The vibrational contribution was calculated in the harmonic approximation (Gordy, Cook &

Weissberger 1984), as we proceeded in our previous studies (see e.g. Margulès et al. 2020). The four lowest vibrational excited states levels were considered. The remaining ones above 870 cm⁻¹ (1252 K) were found to have no influence on the partition function calculations especially at temperatures below 200 K. The band centres values were taken from table 3 in Dalbouha et al. (2017).

Table 6. Rotational, vibrational, and total partition functions of 2-hydroxyacetonitrile isotopologues at various temperatures.

| $T(K)$ | $\text{HO}^{13}\text{CH}_2\text{CN}$ | | | $\text{HOCH}_2^{13}\text{CN}$ | | | DOCH_2CN | | |
|--------|--------------------------------------|---------------------|-----------------------|-------------------------------|---------------------|-----------------------|--------------------------|---------------------|-----------------------|
| | $Q_{\text{rot}}(T)$ | $Q_{\text{vib}}(T)$ | $Q_{\text{tot}}(T)^a$ | $Q_{\text{rot}}(T)$ | $Q_{\text{vib}}(T)$ | $Q_{\text{tot}}(T)^a$ | $Q_{\text{rot}}(T)$ | $Q_{\text{vib}}(T)$ | $Q_{\text{tot}}(T)^a$ |
| 300 | 66349.366 | 2.945 | 195427.600 | 65599.953 | 2.983 | 195705.692 | 70508.718 | 3.448 | 243084.660 |
| 225 | 43025.987 | 1.938 | 83402.987 | 42538.671 | 1.955 | 83169.251 | 45852.122 | 2.201 | 100939.594 |
| 150 | 23269.950 | 1.316 | 30624.476 | 23005.366 | 1.321 | 30395.412 | 24923.049 | 1.428 | 35588.472 |
| 75 | 8080.026 | 1.028 | 8303.656 | 7987.232 | 1.028 | 8212.221 | 8781.574 | 1.047 | 9198.324 |
| 37.5 | 2762.515 | 1.000 | 2763.682 | 2730.231 | 1.000 | 2731.423 | 3088.620 | 1.001 | 3092.371 |
| 18.75 | 917.588 | 1.000 | 917.588 | 906.545 | 1.000 | 906.545 | 1081.656 | 1.000 | 1081.657 |
| 9.375 | 290.775 | 1.000 | 290.775 | 287.126 | 1.000 | 287.126 | 375.515 | 1.000 | 375.515 |

Note. ^a $Q_{\text{tot}}(T)$ values are calculated without truncation of $Q_{\text{rot}}(T)$ and $Q_{\text{vib}}(T)$ at the third digit.

4 ASTRONOMICAL OBSERVATIONS: SEARCH FOR HYDROXYACETONITRILE ISOTOPOLOGUES IN SMM1-A AND IRAS 16293 B

4.1 SMM1-a

The main isotopologue of hydroxyacetonitrile has been detected towards Serpens SMM1-a (hereafter SMM1-a) at high abundance (Ligterink et al. 2021), making this a suitable target to search for its isotopologues DOCH_2CN , $\text{HO}^{13}\text{CH}_2\text{CN}$, and $\text{HOCH}_2^{13}\text{CN}$. The source, observations, and methods are described in Ligterink et al. (2021) and therefore be covered briefly here. SMM1 is a well-characterized and chemically rich source, located at a distance of 436 ± 10 pc (Ortiz-León et al. 2017), and consists of multiple protostars. The brightest, SMM1-a, is an intermediate-mass Class 0 protostar. Recently, this source was targeted with ALMA towards a phase centre of $\alpha_{J2000} = 18:29:49.80$, $\delta_{J2000} = +01:15:20.6$. Selected frequency windows in Band 6 between 217 and 235 GHz were targeted. A synthetic beam of ~ 1.2 arcsec was employed, which is insufficient to resolve the hot corino. Analysis of an extracted spectrum towards the SMM1-a continuum peak in a single beam with the CASSIS³ line analysis software resulted in the detection of several prebiotic molecules, including HOCH_2CN . Hydroxyacetonitrile was detected at $N_{\text{Tot}} = (7.4 \pm 0.9) \times 10^{14} \text{ cm}^{-2}$, $T_{\text{ex}} = 260 \pm 45 \text{ K}$, $\Delta V = 2.5 \pm 0.3 \text{ km s}^{-1}$, and $V_{\text{LSR}} = 6.8 \pm 0.2 \text{ km s}^{-1}$ (Ligterink et al. 2021). To identify the isotopologues, their lines are searched within a 3 S/N detection. Upon identification, a synthetic spectrum is fitted to these lines, assuming local thermodynamic equilibrium (LTE) conditions. If no lines are detected, the upper limit column density of an isotopologue is determined in line-free spectral regions where a transition of said isotopologue is located. The parameters T_{ex} , ΔV , and V_{LSR} are adopted from the main isotopologue. In the SMM1-a spectra, the three hydroxyacetonitrile isotopologues are not detected. Several of their undetected transitions are presented in Figs 1, 2, and 3, for DOCH_2CN , $\text{HO}^{13}\text{CH}_2\text{CN}$ and $\text{HOCH}_2^{13}\text{CN}$, respectively. Due to the line-richness of the spectrum, it is difficult to find completely line-free spectral regions. For $\text{HO}^{13}\text{CH}_2\text{CN}$, blended line features seem to be present in the observed spectrum, but these can both be attributed to CH_3COOH . The $26_{2,25} \leftarrow 25_{2,24}$ transition of the synthetic $\text{HOCH}_2^{13}\text{CN}$ spectrum blends in the wing with a CH_3CDO line in the observed spectrum. Due to the issues in determining line-free spectral regions, a conservative estimate of the upper limit

³Based on analysis carried out with the CASSIS software (<http://cassis.irap.omp.eu>; (Vastel et al. 2015) and JPL data base for molecular spectroscopy (Pickett et al. 1998) and the Cologne Database for Molecular Spectroscopy (Müller et al. 2001, 2005; Endres et al. 2016). CASSIS has been developed by IRAP-UPS/CNRS.

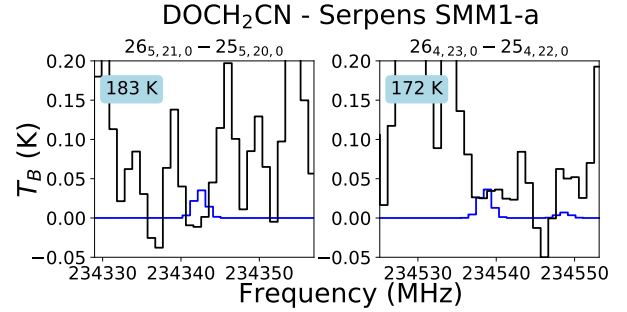


Figure 1. ALMA spectrum of SMM1-a (black) and a synthetic spectrum of DOCH_2CN (blue). Two undetected and largely unblended transitions are shown from which the upper limit column density of $\leq 1 \times 10^{14} \text{ cm}^{-2}$ is determined. Other synthetic spectrum parameters are adopted from the main isotopologue HOCH_2CN detection towards SMM1-a and are fixed at $T_{\text{ex}} = 260 \text{ K}$, $\Delta V = 2.5 \text{ km s}^{-1}$, and $V_{\text{LSR}} = 6.8 \text{ km s}^{-1}$. The upper state energy of each transition is indicated in the top left corner.

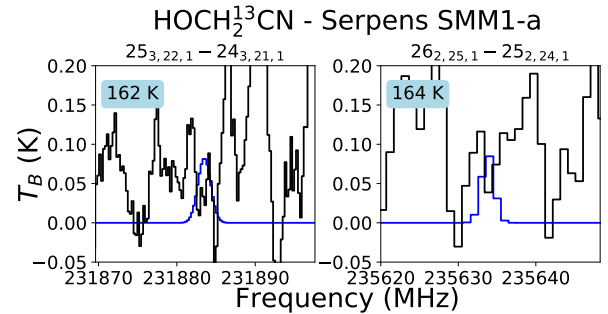


Figure 2. ALMA spectrum of SMM1-a (black) and a synthetic spectrum of $\text{HOCH}_2^{13}\text{CN}$ (blue). Two undetected and largely unblended transitions are shown from which the upper limit column density of $\leq 2 \times 10^{14} \text{ cm}^{-2}$ is determined. Other synthetic spectrum parameters are adopted from the main isotopologue HOCH_2CN detection towards SMM1-a and are fixed at $T_{\text{ex}} = 260 \text{ K}$, $\Delta V = 2.5 \text{ km s}^{-1}$, and $V_{\text{LSR}} = 6.8 \text{ km s}^{-1}$. The upper state energy of each transition is indicated in the top left corner. The $26_{2,25} \hat{a} 25_{2,24}$ transition is blended in the wing with a CH_3CDO transition.

column density is given. For DOCH_2CN $N_{\text{tot}} \leq 1 \times 10^{14} \text{ cm}^{-2}$, while for both ^{13}C isotopologues it is set a $N_{\text{tot}} \leq 2 \times 10^{14} \text{ cm}^{-2}$. This results in (isotopologue)/(HOCH_2CN) ratios of ≤ 0.14 and ≤ 0.27 for the deuterated and ^{13}C hydroxyacetonitrile isotopologues, respectively (see Table 7). Part of the reason that the isotopologues of HOCH_2CN are not detected lies in the fact that the spectral windows of the SMM1-a observations miss the most of the strongest transitions of these species. Fig. 4 shows the normalized synthetic spectra of DOCH_2CN , $\text{HO}^{13}\text{CH}_2\text{CN}$, and $\text{HOCH}_2^{13}\text{CN}$ at $T_{\text{ex}} = 260 \text{ K}$, with the

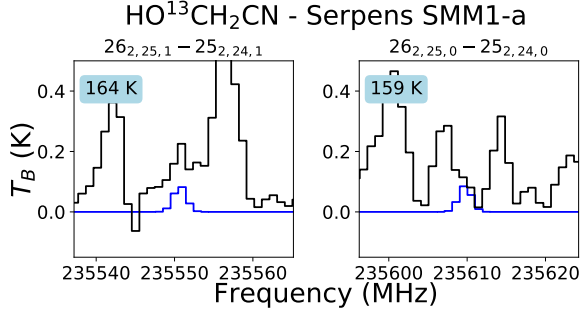


Figure 3. *ALMA* spectrum of SMM1-a (black) and a synthetic spectrum of HO¹³CH₂CN (blue). Two undetected and largely unblended transitions are shown from which the upper limit column density of $\leq 2 \times 10^{14}$ cm⁻² is determined. Other synthetic spectrum parameters are adopted from the main isotopologue HOCH₂CN detection towards SMM1-a and are fixed at $T_{\text{ex}} = 260$ K, $\Delta V = 2.5$ km s⁻¹, and $V_{\text{LSR}} = 6.8$ km.s⁻¹. The upper state energy of each transition is indicated in the top-left corner. Both transitions are blended with CH₃COOH lines.

Table 7. Derived isotopic ratios towards IRAS 16293 B and SMM1-a.

| Source | SMM1-a | IRAS 16293 B |
|----------------------------------|-------------|--------------|
| ¹³ C/ ¹² C | ≤ 0.27 | ≤ 0.5 |
| D/H | ≤ 0.14 | ≤ 0.5 |

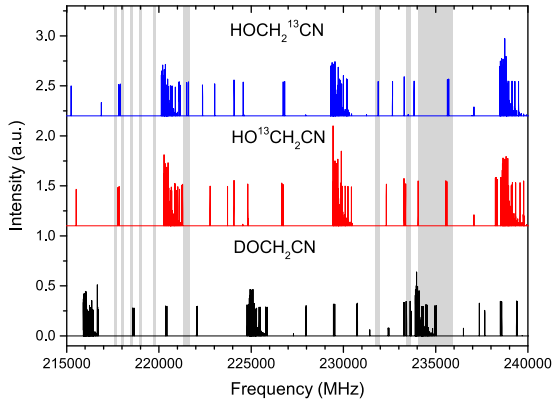


Figure 4. Normalized synthetic spectra of HOCH₂¹³CN (blue), HO¹³CH₂CN (red), and DOCH₂CN (black) for $T_{\text{ex}} = 260$ K, $\Delta V = 2.5$ km s⁻¹, and $V_{\text{LSR}} = 6.8$ km s⁻¹ together with the locations of the spectral windows of the SMM1-a observations (grey). With the exception of a number of DOCH₂CN lines covered by the continuum window, the strongest and most prominent transitions of these hydroxyacetonitrile isotopologues are not covered by the observations.

location of the spectral windows indicated. Only several DOCH₂CN lines are covered in the low-resolution continuum band between 234.06 and 235.93 GHz. Follow-up observations with ALMA that target the strongest isotopologue transition at higher sensitivity will presumably be more successful in detecting these species.

4.2 IRAS 16293 B

HOCH₂CN has also been detected towards the low-mass protostar IRAS 16293 B (Zeng et al. 2019; Ligterink et al. 2021). Contrary to SMM1-a, a large spectral range (329–363 GHz) has been covered for this source in the framework of the *ALMA*-PILS survey, which is fully described in Jørgensen et al. (2016). Faint lines of

hydroxyacetonitrile lines were identified at the so-called half-beam offset position (Ligterink et al. 2021). We consequently searched for the ¹³C isotopologues at the same position. No lines of the ¹³C isotopologues are detected. Assuming an excitation temperature of 150 K (similar to the one obtained by Zeng et al. 2019), a source size of 0.5 arcsec, a linewidth $\Delta V = 1$ km s⁻¹, and a $V_{\text{LSR}} = 2.7$ km s⁻¹, we derive an upper limit of 1.5×10^{15} cm⁻² for both HO¹³CH₂CN and HOCH₂¹³CN. The upper limit would be lower if the excitation temperature is higher. Using the column density of 3×10^{15} cm⁻² derived for the main isotopologue by Ligterink et al. (2021), we obtain a ¹³C/¹²C ≤ 0.5 (see Table 7). DOCH₂CN was also searched for in the PILS survey but is undetected with a column density lower than 1.5×10^{15} cm⁻² for $T_{\text{ex}} = 150$ K. This leads to an upper limit for the D/H ratio of 50 per cent (see Table 7), which is well above the values derived for the mono-deuterated isotopologues of other complex organic molecules in this source with the same survey: 1–8 per cent (Coutens et al. 2016, 2018; Jørgensen et al. 2018; Persson et al. 2018; Müller et al. 2023). Given the lower constraints obtained for IRAS 16293 B and the small spectral range covered by the observations of SMM1-a so far, it appears that SMM1-a would be a better target for follow-up observations.

As Zeng et al. (2019) identified clearer lines of HOCH₂CN towards IRAS 16293 B with larger angular resolution observations, we also checked the *ALMA* archive data with angular sizes between 1 and 2 arcsec. We used the ATOMIS⁴ web application to search for the three isotopologues in the archival *ALMA* data with the following request: an angular resolution between 1 and 2 arcsec, a spectral resolution better than 0.5 km s⁻¹, and a sensitivity better than 6 mJy beam⁻¹ for a bin width of 1 km s⁻¹. We restricted the search to the Bands 3, 4, 5, and 6 similarly to Zeng et al. (2019) and we only looked at the transitions with an A_{ij} higher than 5×10^{-5} s⁻¹. We found that one transition of HOCH₂¹³CN and two transitions of HO¹³CH₂CN at 139.5831, 139.6833, and 139.8175 GHz, respectively, are covered in the project 2013.1.00352.S. Multiple transitions of DOCH₂CN are covered in the project 2018.1.01496.S. We visualize the fits cubes provided on the *ALMA* archive with ALADIN⁵ and CASSIS. The HOCH₂¹³CN line at 139.5831 GHz is blended with a CH₃COCH₃ line. The two transitions of HO¹³CH₂CN are within the noise. No DOCH₂CN line is detected either. This confirms that SMM1-a could be a better target for future studies.

5 CONCLUSION

Millimetre and submillimetre wave spectra of three 2-hydroxyacetonitrile isotopologues, HO¹³CH₂CN, HOCH₂¹³CN, and DOCH₂CN, were assigned up to 530 GHz. This has allowed us to produce accurate predictions of the spectra and made possible a search for these isotopologues in the ISM. Only non-detections could be reported in this work toward SMM1-a and IRAS 16293 B with no significant constraints on the ¹³C/¹²C and D/H ratios of this molecule. The spectroscopic predictions are now available to the astrophysical community, enabling future searches for these 2-hydroxyacetonitrile isotopologues as more sensitive surveys become available.

⁴ATOMIS (*ALMA* archive Tool for Molecular Investigations in Space) is developed at IRAP-UPS/CNRS in the framework of the ERC starting grant Chemtrip (grant agreement No. 949278).

⁵<https://aladin.u-strasbg.fr/AladinDesktop/> (The principal authors are listed below without forgetting many contributors: Pierre Fernique, Thomas Boch, Anaïs Oberto, François Bonnarel, Chaitra, Caroline Bot).

ACKNOWLEDGEMENTS

This work was supported by the CNRS through the MITI interdisciplinary programmes. AC received financial support from the European Research Council (ERC) under the European Unions Horizon 2020 research and innovation programme (ERC Starting Grant Chemtrip, grant agreement no. 949278). JCG thanks the Centre National d'Etudes Spatiales (CNES) for a grant. NFWL acknowledges funding by the Swiss National Science Foundation Ambizione grant 193453. This paper makes use of the following *ALMA* data: ADS/JAO.ALMA2013.1.00278.S, ADS/JAO.ALMA2018.1.00836.S, and ADS/JAO.ALMA2013.1.00352.S. *ALMA* is a partnership of ESO (representing its member states), NSF (USA), and NINS (Japan), together with NRC (Canada), NSC and ASIAA (Taiwan), and KASI (Republic of Korea), in cooperation with the Republic of Chile. The Joint *ALMA* Observatory is operated by ESO, AUI/NRAO, and NAOJ.

DATA AVAILABILITY

Owing to their large size, the complete versions of the global fit (Tables S1, S2, and S3) for the three isotopologues are supplied at the CDS.⁶ The predicted spectra are available in different formats including STANDARD.CAT format (Pickett 1972) from the new data base of the Lille spectroscopy group called the Lille Spectroscopic Database.⁷

REFERENCES

- Cazzoli G., Lister D., Mirri A., 1973, *J. Chem. Soc., Faraday Trans. 2*, 69, 569
- Christen D., Müller H. S., 2003, *Phys. Chem. Chem. Phys.*, 5, 3600
- Coudert L., Hougen J., 1988, *J. Mol. Spectrosc.*, 130, 86
- Coutens A. et al., 2016, *A&A*, 590, L6
- Coutens A. et al., 2018, *A&A*, 612, A107
- Dalbouha S., Domínguez-Gómez R. M., Senent M. L., 2017, *Eur. Phys. J. D*, 71, 161
- Danger G., Duvernay F., Theulé P., Borget F., Chiavassa T., 2012, *ApJ*, 756, 11
- Endres C. P., Schlemmer S., Schilke P., Stutzki J., Müller H. S., 2016, *J. Mol. Spectrosc.*, 327, 95
- Gaudry R., 1947, *Org. Synth.*, 27, 41
- Gaudry R., 1955, *Org. Synth.*, 3, 436

⁶<https://cds.unistra.fr> (description of the VizieR service was published in 2000, *A&AS* 143, 23).

⁷<https://ltd.univ-lille.fr> (Lille Spectroscopic Database is created and maintained by Roman Motiyenko and Laurent Margulès).

- Gordy W., Cook R. L., Weissberger A., 1984, *Microwave Molecular Spectra*, Vol. 18. Wiley, New York
- Halfen D. T., Woolf N. J., Ziurys L. M., 2017, *ApJ*, 845, 158
- Hougen J. T., 1985, *J. Mol. Spect.*, 114, 395
- Jacob A. M., Menten K. M., Wiesemeyer H., Güsten R., Wyrowski F., Klein B., 2020, *A&A*, 640, A125
- Jørgensen J. K. et al., 2016, *A&A*, 595, A117
- Jørgensen J. K. et al., 2018, *A&A*, 620, A170
- Ligterink N. F. W. et al., 2021, *A&A*, 647, A87
- Margulès L., McGuire B. A., Senent M. L., Motiyenko R. A., Remijan A., Guillemin J. C., 2017, *A&A*, 601, A50
- Margulès L., McGuire B. A., Evans C. J., Motiyenko R. A., Remijan A., Guillemin J. C., Wong A., McNaughton D., 2020, *A&A*, 642, A206
- Motiyenko R. A., Margulès L., Goubet M., Møllendal H., Kononov A., Guillemin J.-C., 2010, *J. Phys. Chem. A*, 114, 2794
- Motiyenko R. A., Margulès L., Alekseev E. A., Guillemin J.-C., 2015, *J. Phys. Chem. A*, 119, 1048
- Motiyenko R. A., Margulès L., Senent M. L., Guillemin J.-C., 2018, *J. Phys. Chem. A*, 122, 3163
- Müller H. S. P., Thorwirth S., Roth D. A., Winnewisser G., 2001, *A&A*, 370, L49
- Müller H. S., Schlöder F., Stutzki J., Winnewisser G., 2005, *J. Mol. Struct.*, 742, 215
- Müller H. S., Belloche A., Menten K. M., Comito C., Schilke P., 2008, *J. Mol. Spect.*, 251, 319
- Müller H. S. P., Jørgensen J. K., Guillemin J.-C., Lewen F., Schlemmer S., 2023, *MNRAS*, 518, 185
- Ortiz-León G. N. et al., 2017, *ApJ*, 834, 143
- Parise B., Castets A., Herbst E., Caux E., Ceccarelli C., Mukhopadhyay I., Tielens A. G. G. M., 2004, *A&A*, 416, 159
- Persson M. V. et al., 2018, *A&A*, 610, A54
- Pickett H. M., 1972, *J. Chem. Phys.*, 56, 1715
- Pickett H. M., 1991, *J. Mol. Spectrosc.*, 148, 371
- Pickett H., Poynter R., Cohen E., Delitsky M., Pearson J., Müller H., 1998, *J. Quant. Spec. Radiat. Transf.*, 60, 883
- Roueff E., Lis D. C., van der Tak F. F. S., Gerin M., Goldsmith P. F., 2005, *A&A*, 438, 585
- Schwartz A. W., Goverde M., 1982, *J. Mol. Evol.*, 18, 351
- Smirnov I., Alekseev E., Piddyachiy V., Ilyushin V., Motiyenko R., 2013, *J. Mol. Spectrosc.*, 293, 33
- Vastel C., Bottinelli S., Caux E., Glorian J., Boiziot M., 2015, in Martins F., Boissier S., Buat V., Cambrésy L., Petit P., eds, SF2A-2015: Proceedings of the Annual Meeting of the French Society of Astronomy and Astrophysics. Toulouse, France, p. 313
- Wilson T. L., Rood R. T., 1994, *ARA&A*, 32, 191
- Zakharenko O., Motiyenko R. A., Margulès L., Huet T. R., 2015, *J. Mol. Spect.*, 317, 41
- Zeng S., Quénard D., Jiménez-Serra I., Martí n Pintado J., Rivilla V. M., Testi L., Martí n-Domé nech R., 2019, *MNRAS*, 484, L43

This paper has been typeset from a $\text{\TeX}/\text{\LaTeX}$ file prepared by the author.